

## Tweaking the Charge Transfer: Bonding Analysis of Bismuth(III) Complexes with a Flexidentate Phosphane Ligand

Réka Mokrai, Jamie Barrett, David C. Apperley, Zoltán Benkő,\* and Dominikus Heift\*

Cite This: *Inorg. Chem.* 2020, 59, 8916–8924

Read Online

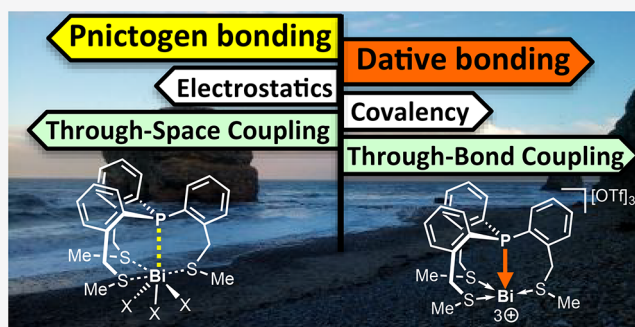
ACCESS |

Metrics & More

Article Recommendations

Supporting Information

**ABSTRACT:** To account for the charge transfer and covalent character in bonding between P and Bi centers, the electronic structures of  $[P(C_6H_4-o-CH_2SCH_3)_3BiCl_n]^{(3-n)+}$  ( $n = 0-3$ ) model species have been investigated computationally. On the basis of this survey a synthetic target compound with a dative  $P \rightarrow Bi$  bond has been selected. Consecutively, the highly reactive bismuth cage  $[P(C_6H_4-o-CH_2SCH_3)_3Bi]^{3+}$  has been accessed experimentally and characterized. Importantly, our experiments (single-crystal X-ray diffraction and solid-state NMR spectroscopy) and computations (NBO and AIM analysis) reveal that the  $P \cdots Bi$  bonding in this trication can be described as a dative bond. Here we have shown that our accordion-like molecular framework allows for tuning of the interaction between P and Bi centers.



### 1. INTRODUCTION

The hundred years old concept of coordinative covalent or dative bonding has evolved from a fundamental physical theory<sup>1,2</sup> to cornerstones of undergraduate chemical education. In contrast to electron-sharing covalent bonding, dative bonding arises between two closed-shell systems, an electron pair donor (Lewis base) and an electron pair acceptor (Lewis acid), and significant electron density is transferred from the donor to the acceptor (charge transfer). More recently, the concept of  $\sigma$ -hole interactions introduced just a decade ago<sup>3,4</sup> has gained increasing attention<sup>5-7</sup> (note that some examples such as hydrogen bonds and halogen bonds have been known for much longer<sup>5</sup>).  $\sigma$ -Hole interactions, similarly to dative bonds, also arise between two closed-shell entities, but they are regarded as noncovalent in nature. A relatively new congener of noncovalent interactions is the pnictogen bond (PnB),<sup>8-10</sup> which (in analogy with the IUPAC definition of a halogen bond<sup>11</sup>) can be defined as an attractive interaction between the electron-deficient region of a pnictogen (group 15 element) called a pnictogen bond donor and a Lewis base (pnictogen bond acceptor, acting as an electron pair donor).<sup>12</sup> In the past few years, the potential of PnB in structural assembly, supramolecular architecture, anion sensing, (organo)catalysis, and molecular recognition has also been highlighted.<sup>7,13-21</sup> On the basis of thorough computational studies,<sup>6,9,22-41</sup> pnictogen bonding is chiefly electrostatic in nature (attraction between the oppositely charged regions around the two centers). Moreover, charge transfer effects (donation from the lone pair of the Lewis base into the  $\sigma^*$ -antibonding orbitals at the pnictogen center) may also contribute, though to a much lesser extent. This also means that the charge transfer and thus the

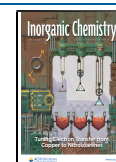
covalent character in pnictogen bonding are rather low. Importantly, the strength of a pnictogen interaction can be comparable to that of a hydrogen bond. However, the experimental observation is still challenging, especially with spectroscopic methods such as NMR spectroscopy.<sup>9,15,42-45</sup>

Even though the concepts of both dative bonds and  $\sigma$ -hole interactions are well-known, to our knowledge the relationship and connectivity between them has not yet been explored experimentally. In the present study we aim to investigate the bonding situation in P/Bi complexes. Due to its highest polarizability among the group 15 elements, bismuth has the strongest ability to form complexes with conventional dative bonds. On the other hand, phosphorus stands out because of its excellent NMR properties (broad chemical shift range, 100% natural abundance) and can be employed as a sensor to detect delicate structural changes.

Several prototype donor–acceptor complexes are known in the literature exhibiting P–Bi distances described as dative bonds such as the *peri*-substituted acenaphthyl derivative **A** (2.7696(8) Å)<sup>46</sup> and other recently reported congeners of this family<sup>47</sup> and the monocation **B** shown in Figure 1 (2.6883(14) and 2.6750(13) Å).<sup>48</sup> Similarly, a dative bond was reported for a phosphane coordinated diphenylbismuth-

Received: March 11, 2020

Published: June 12, 2020



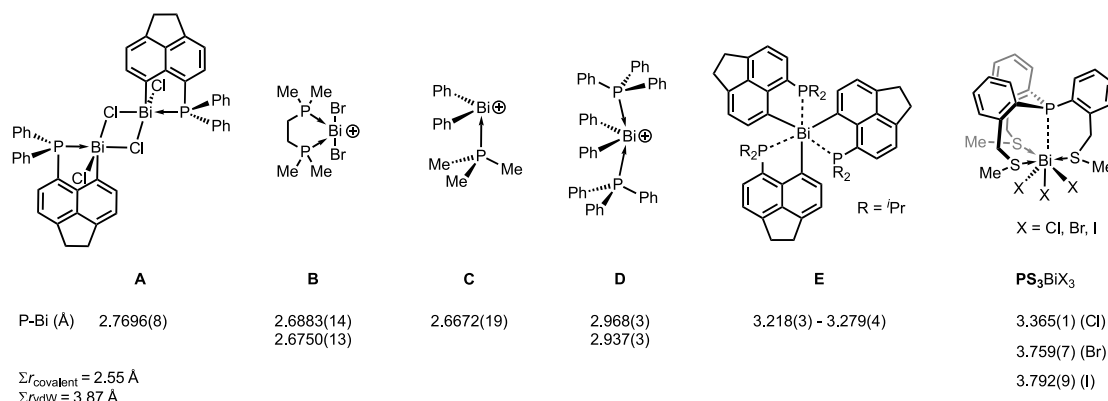


**Figure 1.** Selected examples of P–Bi distances determined by X-ray crystallography. For **B**, **C** and **D** the counteranions are not shown.  $\Sigma r_{\text{covalent}}$  and  $\Sigma r_{\text{vdW}}$  denote the sum of covalent<sup>53</sup> and van der Waals<sup>54</sup> radii, respectively, for the P–Bi couple.

mium cation (see **C** 2.6672(19) Å).<sup>49</sup> In contrast, significantly longer P–Bi distances of 2.968(3) and 2.937(3) Å were observed for the related complex **D**, in which two phosphane ligands coordinate to the bismuthenium cation. These bonds were described rather as an electrostatic, induced dipole–ion attraction than a conventional dative bond.<sup>50</sup> The Bi...P distance can be stretched further as in the geminally substituted tris(acenaphthyl) bismuthine **E** (3.218(3)–3.279(4) Å), in which only weak interactions between the P and Bi centers were found.<sup>51</sup> Recently we have reported a series of phosphane–trihalobismuth complexes ( $\text{PS}_3\text{BiX}_3$ , X = Cl, Br, I), featuring even longer P...Bi distances (in the range of 3.365(1)–3.792(9) Å). The interactions between the P and Bi centers in these  $\text{PS}_3\text{BiX}_3$  compounds exhibit a remarkable strength of 7.1–8.8 kcal mol<sup>−1</sup>.<sup>52</sup>

The goal of the present study is to gain more insight into the bonding situation in bismuth(III) complexes with the  $\text{PS}_3$  ligand. Although other multidentate ligand systems are known in the literature,<sup>55–64</sup> due to their accordion-like structural flexibility the molecular skeleton of type  $\text{PS}_3\text{BiX}_3$  seems to be suitable for experimental investigations. First, we aim to predict computationally how the pnictogen interaction between the bridgehead atoms P and Bi observed in the neutral  $\text{PS}_3\text{BiX}_3$  compounds can be shifted into a dative (covalent) regime, and subsequently, we provide experimental evidence based on X-ray crystallography and NMR studies.

## 2. RESULTS AND DISCUSSION

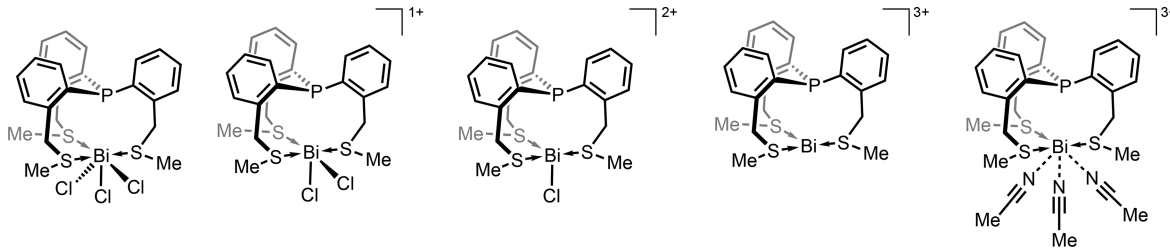
**2.1. Computational Considerations.** To search for possible candidates in which the interaction between the P and Bi can be described with dative bonding, first we investigated a series of species related to  $\text{PS}_3\text{BiX}_3$ . As the P–Bi atom distance in  $\text{PS}_3\text{BiX}_3$  depends on the halide substituent on the bismuth and decreases in the order I > Br > Cl,<sup>52</sup> an obvious choice could be the complex of  $\text{P}(\text{C}_6\text{H}_4\text{-}o\text{-CH}_2\text{SCH}_3)_3$  ( $\text{PS}_3$ ) with bismuth trifluoride; however, this compound could not be synthetically realized due to the extreme low solubility of  $\text{BiF}_3$ .<sup>52</sup> Alternatively, the halides could be changed for weakly coordinating anions. In our computational survey we studied a series of model species arising by sequential abstraction of chlorides from the compound  $\text{PS}_3\text{BiCl}_3$ . Thus, the monocation  $[\text{PS}_3\text{BiCl}_2]^+$ , the dication  $[\text{PS}_3\text{BiCl}]^{2+}$ , the trication  $[\text{PS}_3\text{Bi}]^{3+}$ , and the complex of the trication with three acetonitrile (ACN) molecules,  $[\text{PS}_3\text{Bi}(\text{ACN})_3]^{3+}$  were investigated alongside the neutral compound  $\text{PS}_3\text{BiCl}_3$ . In order to gain insight into the bonding situation between the P and Bi

atoms we performed dispersion-corrected DFT calculations (for details and the results at the B3LYP-D3/cc-pVDZ(-PP) level, see the [Supporting Information](#)). Herein, we present the results obtained at the  $\omega\text{B97XD/cc-pVDZ(-PP)}$  level, which was successfully employed for similar systems.<sup>52</sup> Furthermore, the solvent effects were simulated with the polarized continuum model (PCM), employing acetonitrile as solvent. On the optimized structures bond valences have been obtained according to the method described by Brown,<sup>65</sup> employing the data set reported by Brese and O’Keeffe.<sup>66</sup> Furthermore, NBO (natural bonding orbital) computations<sup>67</sup> delivering the Wiberg bond indices as well as atoms in molecules (AIM) analyses<sup>68</sup> have been carried out and the results are collected in [Table 1](#). The NPA (natural population analysis) charges show the same tendencies as the AIM charges and, therefore, they can be found in [Table S5](#) in the Supporting Information.

The P...Bi atom distance decreases systematically upon abstraction of the chlorides in the row of  $\text{PS}_3\text{BiCl}_3 \rightarrow [\text{PS}_3\text{Bi}]^{3+}$ , both in the gas-phase calculations and with the PCM solvent model. If these two data sets (without and with solvent model) are compared, the largest difference (0.154 Å) is observed for the neutral  $\text{PS}_3\text{BiCl}_3$ , while the deviation is significantly smaller for the other species. The PCM model results in somewhat shorter P...Bi distances in the case of the neutral  $\text{PS}_3\text{BiCl}_3$  and the monocationic  $[\text{PS}_3\text{BiCl}_2]^+$ , whereas it results in slightly longer distances for the di- and trications. Altogether, the differences between the results obtained with or without the solvent model are much smaller than those resulting from the change in the substituents/charge. Therefore, the general tendencies among the different species are not affected, and in the following we only discuss the parameters computed using the solvent model.

Importantly, the shortest P...Bi distance is found in the trication  $[\text{PS}_3\text{Bi}]^{3+}$  (2.743 Å), being clearly in the range of dative bonds reported for compounds such as **A**, **B**, and **C** (see [Figure 1](#)). As the direct coordination of solvent molecules to the bismuth center may have an effect on the interaction between the P and Bi centers, we have also computed the model species  $[\text{PS}_3\text{Bi}(\text{ACN})_3]^{3+}$ . As expected, the competition between the donor atoms around the Bi center leads to an elongation of the P...Bi distance (2.849 Å in  $[\text{PS}_3\text{Bi}(\text{ACN})_3]^{3+}$ ). This bond, however, is significantly shorter than that in the dication (2.923 Å in  $[\text{PS}_3\text{BiCl}]^{2+}$ ), and thus the effect of three coordinating solvent molecules is inferior to that of one chloride anion.

Table 1. Calculated Bi...P Atomic Distances ( $d$ , Å) in  $[\text{PS}_3\text{BiCl}_n]^{3-n}$  ( $n = 0-3$ ) and  $[\text{PS}_3\text{Bi}(\text{ACN})_3]^{3+}$ , bond valences ( $s$ , valence units), Wiberg bond indices (WBIs), AIM Charges ( $q$ , electron) and Net Charge Donation from the Ligand to the  $[\text{BiCl}_n]^{3-n}$  moiety ( $\Delta q$  Calculated As the Sum of Partial AIM Charges in the Ligand Fragment), Properties at the Bond Critical Point of Electron Density ( $\rho_{\text{bcp}}$ ,  $\text{e}/\text{\AA}^3$ ), Laplacian of the Electron Density ( $\nabla^2\rho_{\text{bcp}}$ ,  $\text{e}/\text{\AA}^5$ ), Total Electronic Energy Density ( $H$ , au), and Ratio of Potential and Kinetic Energy Density ( $|V|/G$ )<sup>a</sup>



	$\text{PS}_3\text{BiCl}_3$	$[\text{PS}_3\text{BiCl}_2]^+$	$[\text{PS}_3\text{BiCl}]^{2+}$	$[\text{PS}_3\text{Bi}]^{3+}$	$[\text{PS}_3\text{Bi}(\text{ACN})_3]^{3+}$
$d(\text{Bi}-\text{P})$	3.576 3.422	3.058 3.001	2.909 2.923	2.697 2.743	2.817 2.849
$s(\text{Bi}-\text{P})$	0.077 0.118	0.315 0.367	0.470 0.452	0.835 0.737	0.603 0.554
WBI(Bi-P)	0.085 0.145	0.302 0.358	0.417 0.415	0.788 0.715	0.598 0.544
$q(\text{P})$	1.695 1.693	1.722 1.736	1.751 1.756	1.924 1.867	1.795 1.782
$q(\text{Bi})$	1.564 1.588	1.473 1.499	1.333 1.424	1.125 1.337	1.479 1.561
$\Delta q$	0.258 0.432	0.724 0.824	1.224 1.215	1.875 1.663	1.326 1.216
$\rho_{\text{bcp}}$	0.088 0.117	0.226 0.252	0.303 0.294	0.465 0.424	0.370 0.343
$\nabla^2\rho_{\text{bcp}}$	0.643 0.774	1.176 1.183	1.265 1.236	0.333 0.697	0.933 1.068
$H$	$+6.2 \cdot 10^{-4}$ $+2.2 \cdot 10^{-4}$	$-3.3 \cdot 10^{-3}$ $-4.7 \cdot 10^{-3}$	$-7.8 \cdot 10^{-3}$ $-7.2 \cdot 10^{-3}$	$-2.1 \cdot 10^{-2}$ $-1.7 \cdot 10^{-2}$	$-1.3 \cdot 10^{-2}$ $-1.0 \cdot 10^{-2}$
$ V /G$	0.897 0.971	1.214 1.275	1.372 1.358	1.861 1.704	1.566 1.486
$\Sigma s$ at Bi	2.955 2.793	2.824 2.700	2.800 2.575	2.467 2.267	2.609 2.674

<sup>a</sup>The gas-phase data without PCM for  $\text{PS}_3\text{BiCl}_3$  are taken from ref 52. All data were obtained at the  $\omega\text{B97XD/cc-pVDZ(-PP)}$  level of theory. The values obtained with the solvent model PCM are shown in italics.

The strengthening of the interaction between the P and Bi centers in the sequence of  $\text{PS}_3\text{BiCl}_3$ ,  $[\text{PS}_3\text{BiCl}_2]^+$ ,  $[\text{PS}_3\text{BiCl}]^{2+}$ ,  $[\text{PS}_3\text{Bi}(\text{ACN})_3]^{3+}$ , and  $[\text{PS}_3\text{Bi}]^{3+}$  is also reflected in the increasing bond valence values ( $s$ ) and Wiberg bond indices (WBI). These two nicely correlating parameter sets indicate a tendentious rise in covalent character on going from the neutral to the tricationic species. Surprisingly, the AIM charge at the bismuth center shows a decreasing trend upon abstraction of the chlorides, which is moderate if the solvent model is employed and is more pronounced in the gas-phase calculations. This descending charge can be explained by substantial charge transfer from the  $\text{PS}_3$  ligand toward the bismuth center reaching  $\Delta q = 1.875$  e in the gas phase ( $\Delta q = 1.663$  e with the PCM solvent model) for  $[\text{PS}_3\text{Bi}]^{3+}$ . The intensification of the charge transfer is also nicely visible on the AIM charges at the phosphorus centers, which gradually grow

from the neutral  $\text{PS}_3\text{BiCl}_3$  ( $q(\text{P}) = 1.695$  e in the gas phase, 1.693 e with PCM) to the tricationic  $[\text{PS}_3\text{Bi}]^{3+}$  ( $q(\text{P}) = 1.924$  e in the gas phase, 1.867 e with PCM).

The results of the NBO investigations and partial charges are further bolstered by an atoms in molecules (AIM) analysis<sup>68</sup> of the electron density, which located bond critical points (bcp) between the P and Bi nuclei in each of the complexes. The trend of the electron density at the bond critical points ( $\rho_{\text{bcp}}$ ) again indicates gradual strengthening of the interaction between the P and Bi atoms from  $\text{PS}_3\text{BiCl}_3$  to  $[\text{PS}_3\text{Bi}]^{3+}$ . The Laplacian of the electron density at the P...Bi bcp ( $\nabla^2\rho_{\text{bcp}}$ ) is positive for each of these complexes, which suggests closed-shell interactions (dative, ionic, or  $\sigma$ -hole interaction). The electron density and its Laplacian at the bcp of the Bi-P bond in the tricationic  $[\text{PS}_3\text{Bi}]^{3+}$  (0.424  $\text{e}/\text{\AA}^3$  and 0.697  $\text{e}/\text{\AA}^5$ , respectively) are similar to those reported for the acenaphthyl



derivative **A** in Figure 1 ( $0.42 \text{ e}/\text{\AA}^3$  and  $0.6 \text{ e}/\text{\AA}^5$ , respectively<sup>46</sup>), which was described with a polar covalent Bi–P interaction. While the Cl–Bi–Cl arrangement in **A** is close to linear ( $174.32(2)^\circ$ ), a second rotamer exhibiting a pyramidalized Bi environment and an elongated Bi–P bond ( $3.005 \text{ \AA}$ ) could also be optimized. The Bi–P interaction in the latter rotamer was described as rather ionic (electrostatic), and its characteristics ( $\rho_{\text{bcp}} = 0.24 \text{ e}/\text{\AA}^3$  and  $\nabla^2\rho_{\text{bcp}} = 1.0 \text{ e}/\text{\AA}^5$ ) are similar to those of the monocationic  $[\text{PS}_3\text{BiCl}_2]^+$  ( $\rho_{\text{bcp}} = 0.252 \text{ e}/\text{\AA}^3$  and  $\nabla^2\rho_{\text{bcp}} = 1.183 \text{ e}/\text{\AA}^5$ ).

The neutral  $\text{PS}_3\text{BiCl}_3$  and the tricationic  $[\text{PS}_3\text{Bi}]^{3+}$  present the two extremes of noncovalent and dative bonding, respectively; however, there is clearly a continuum between them. The gradual conversion of the electrostatic nature of the interaction into covalency is visible in a smooth change of all the bonding descriptors shown in Table 1. The question may arise where the borderline is between weak interaction and dative bonding. Necessarily, this separation is arbitrary and here we refer to a simple tool based on the relative amount of kinetic and potential energy at the bcp (Cremer–Kraka criteria).<sup>69,70</sup> At the bcp of a covalent bond the potential energy density  $V$  (always negative) is more substantial than the kinetic energy density  $G$  (always positive), resulting in a total electronic energy density  $H = V + G < 0$  or alternatively  $|V|/G > 1$ . These characteristics show that the P···Bi interaction in the trichloride  $\text{PS}_3\text{BiCl}_3$  is chiefly electrostatic, whereas the cationic complexes  $[\text{PS}_3\text{BiCl}_n]^{(3-n)+}$  ( $n = 0–2$ ) all exhibit  $H < 0$  and  $|V|/G > 1$ . Thus, in all these cationic species the P···Bi bond has a highly covalent character and can be classified as a dative bond (P→Bi).

On the basis of the results of the above analysis we propose a simple model based on the competing effects of the donor atoms to understand the different P···Bi bonding situations in the complexes outlined in Table 1. To discuss the changes in the coordination sphere of the Bi center, we employ the bond valences obtained from the geometries optimized with the PCM solvent model (see Table 1 and Table S7 in the Supporting Information). The rather strongly donating chloride ligands and the sulfur donors in the coordination sphere around the bismuth center in  $\text{PS}_3\text{BiCl}_3$  hamper the phosphorus from developing significant charge transfer toward the bismuth. Therefore, a weak, mainly electrostatic pnictogen bond can only be formed, which results in a large P···Bi distance. The valence of the bismuth center in  $\text{PS}_3\text{BiCl}_3$  is 2.793 vu (valence units), calculated as the sum of bond valences ( $\sum s$ ). The abstraction of one chloride ligand formally frees up a coordination site by 0.663 vu (taken as the least strongly bound chloride among the three; see Table S7), which initiates reorganization to reach a new equilibrium structure. Thus, the remaining donors can coordinate more strongly to the bismuth, which is reflected in the larger P···Bi and S···Bi bond valences (for details see Table S7 in the Supporting Information) and the valence of the bismuth center is almost re-established ( $\sum s = 2.700 \text{ vu}$  in  $[\text{PS}_3\text{BiCl}_2]^+$ ). Similar phenomena occur for the abstraction of the second and third chloride anions. However, the “buffering effect” of the remaining donors to re-establish the valence of the bismuth center decreases somewhat, which can clearly be seen in the slight gradual dropping of the  $\sum s$  values in the direction  $\text{PS}_3\text{BiCl}_3$  to  $[\text{PS}_3\text{Bi}]^{3+}$  (see Table 1), indicating slight undercoordination. Nevertheless, the intensification of the charge transfer (due to the sequential abstraction of chloride

ions) results in a gradual strengthening of the P···Bi and S···Bi interactions in the same direction.

On the basis of the computations above, all three cationic species seem to be suitable for experimental detection of a dative interaction between the P and Bi centers. However, to target the strongest possible P→Bi interaction, we chose the trication  $[\text{PS}_3\text{Bi}]^{3+}$  with weakly coordinating anions as the best candidate for our experimental study.

**2.3. Experimental Validation.** In order to access the aimed tricationic coordination compound  $[\text{PS}_3\text{Bi}]^{3+}$ , we decided to employ trifluoromethanesulfonate (triflate) as a counteranion for two reasons: the triflate anion is reasonably weakly coordinating,<sup>71</sup> and bismuth triflate is an easily accessible metal salt, which is also widely used as a catalyst in various organic syntheses.<sup>72,73</sup>

To form the target complex, the ligand  $\text{P}(\text{C}_6\text{H}_4\text{-}o\text{-CH}_2\text{SCH}_3)_3$  ( $\text{PS}_3$ )<sup>52</sup> and 1 equiv of commercially available bismuth trifluoromethanesulfonate  $\text{Bi}[\text{OTf}]_3(\text{H}_2\text{O})_n$  ( $n \approx 14$  according to a TGA measurement) were reacted in acetonitrile at room temperature. In the  $^{31}\text{P}\{^1\text{H}\}$  NMR spectrum of this reaction mixture only a singlet at  $-22.0 \text{ ppm}$  was observed, which appears in the  $^{31}\text{P}$  NMR spectrum as a doublet with  $^1J_{\text{PH}} = 535.0 \text{ Hz}$ , indicating protonation at the phosphorus center. This phosphorus-containing product was unambiguously identified by  $^{31}\text{P}$ ,  $^{13}\text{C}$ , and  $^1\text{H}$  NMR spectroscopy and a single-crystal X-ray diffraction study as the phosphonium salt  $[\text{HP}(\text{C}_6\text{H}_4\text{-}o\text{-CH}_2\text{SCH}_3)_3]^+[\text{OTf}]^-$  (see Figure S7 in the Supporting Information). Note that bismuth salts in general are prone to hydrolysis in the presence of water and in this case the hydrolysis of bismuth triflate resulted in the formation of triflic acid, which as a strong acid can protonate the phosphane ligand  $\text{PS}_3$ .

According to the literature it is practically impossible to obtain strictly anhydrous bismuth triflate.<sup>74,75</sup> To decrease the possibility of hydrolysis, we dried  $\text{Bi}[\text{OTf}]_3$  for 10 days at  $160^\circ\text{C}$  under a dynamic vacuum,<sup>76</sup> which resulted in a solid with the formula of  $\text{Bi}[\text{OTf}]_3(\text{H}_2\text{O})_n$  ( $n \approx 2.8$ , on the basis of elemental analysis). We repeated the reaction described above employing  $\text{Bi}[\text{OTf}]_3(\text{H}_2\text{O})_n$  ( $n \approx 2.8$ ) in toluene instead of acetonitrile, which resulted in the formation of a yellow precipitate. On the basis of its solid-state  $^{31}\text{P}$  CP-MAS NMR spectrum this material is a mixture of products. However, recrystallization from acetonitrile delivered yellow crystals isolated in a low yield (15%). These crystals were also suitable for single-crystal X-ray diffraction analysis (see below), showing that their composition is  $[\text{PS}_3\text{Bi}]_2\{\text{Bi}_6\text{O}_4(\text{OH})_4[\text{OTf}]_{12}\}(\text{H}_2\text{O})(\text{CH}_3\text{CN})_6$ , which was also confirmed by elemental analysis of the isolated product.  $[\text{PS}_3\text{Bi}]_2\{\text{Bi}_6\text{O}_4(\text{OH})_4[\text{OTf}]_{12}\}(\text{H}_2\text{O})(\text{CH}_3\text{CN})_6$  is in the following abbreviated as  $[\text{PS}_3\text{Bi}]_2[\text{BOT}]$ , in which the “bismuth oxo triflate” cluster hexaanion  $[\text{BOT}]^{6-}$  stands for  $\{\text{Bi}_6\text{O}_4(\text{OH})_4[\text{OTf}]_{12}\}^{6-}$  (Figure 2). This compound is only stable in the solid state and was further characterized by CP-MAS  $^{31}\text{P}$ ,  $^1\text{H}$ ,  $^{13}\text{C}$ , and  $^{19}\text{F}$  NMR spectroscopy (for details see section 2.5 and Figure 4). The low yield is attributed to the observation that  $[\text{PS}_3\text{Bi}]_2[\text{BOT}]$  decomposes in solution. Indeed, when crystals of  $[\text{PS}_3\text{Bi}]_2[\text{BOT}]$  are dissolved in dry acetonitrile, the  $^{31}\text{P}$  NMR spectrum of the solution (see Figure S2) shows two resonances: a very small singlet resonance at  $\delta +67.6 \text{ ppm}$  is observed (likely indicating the  $[\text{PS}_3\text{Bi}]^{3+}$  species) while the larger doublet resonance at  $\delta -22.0 \text{ ppm}$  with the coupling constant  $^1J_{\text{PH}} = 535.0 \text{ Hz}$  again indicates the

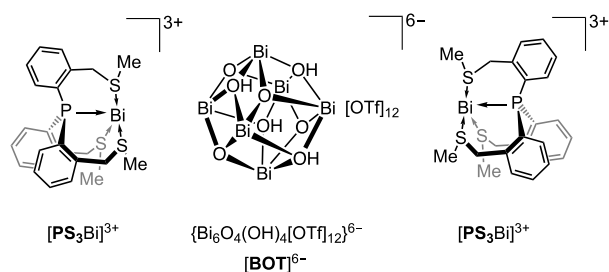


Figure 2. Schematic depiction of  $[\text{PS}_3\text{Bi}]_2[\text{BOT}]$ .

phosphonium salt  $[\text{HPS}_3]^+[\text{OTf}]^-$  as a decomposition product.

**2.4. Structural Studies.** We suggest describing the compound  $[\text{PS}_3\text{Bi}]_2[\text{BOT}]$  as an assembly of two tricationic  $[\text{PS}_3\text{Bi}]^{3+}$  units and a central  $\{\text{Bi}_6\text{O}_4(\text{OH})_4[\text{OTf}]_{12}\}^{6-}$  cluster anion (Figure 3), on the basis of the analogy of the latter to known cluster anions such as  $[\text{Bi}_6\text{O}_4(\text{OH})_4(\text{F}_3\text{CCO}_2)_{12}]^{6-}$ .<sup>77</sup> Alternatively,  $[\text{PS}_3\text{Bi}]_2[\text{BOT}]$  could also be considered as  $\{[\text{PS}_3\text{Bi}][\text{OTf}]_3\}\{\text{Bi}_6\text{O}_4(\text{OH})_4[\text{OTf}]_{12}\}\{[\text{PS}_3\text{Bi}][\text{OTf}]_3\}$  with two neutral capping  $\{[\text{PS}_3\text{Bi}][\text{OTf}]_3\}$  moieties and a central neutral  $\{\text{Bi}_6\text{O}_4(\text{OH})_4[\text{OTf}]_6\}$  cluster.

The so far unknown  $\{\text{Bi}_6\text{O}_4(\text{OH})_4[\text{OTf}]_{12}\}^{6-}$  ( $[\text{BOT}]^{6-}$ ) cluster hexaanion formally consists of a cationic  $[\text{Bi}_6(\mu_3\text{-O})_4(\mu_3\text{-OH})_4]^{6+}$  core surrounded by 12 triflate anions. In the core, which is a common motif in hydrolysis products of bismuth salts,<sup>77–84</sup> six bismuth(III) centers occupy the corners of an octahedron, whose faces are capped by four oxo and four hydroxo ligands in a  $\mu_3$  fashion (the hydroxy protons could not be located crystallographically). The 12 edges of the octahedron are each capped by a triflate anion in a  $\mu_2$ -O fashion, six of which form the ring arrangement shown in Figure 3b. The additional (2 times 3) triflate anions bridge the central core with one of the two tricationic  $[\text{PS}_3\text{Bi}]^{3+}$  moieties on the two sides of the structure (Figure 3a).

The bismuth centers of these  $[\text{PS}_3\text{Bi}]^{3+}$  fragments are coordinated by three triflate anions as well as the three sulfur and the phosphorus centers of ligand  $\text{PS}_3$ ; the  $C_3$  symmetry around the bismuth centers suggests stereochemical inactivity of their lone pairs. The Bi–S atom distances of 2.749(9) Å reflect a dative bond between the sulfur donor and a Bi(III) cation (for example 2.6873(3)–3.013(2) Å in Bi(III) chalcogenone complexes).<sup>85</sup> The Bi–O[triflate] distances (2.760(1) Å) are between the sum of the covalent and van der Waals radii of the respective elements (2.14<sup>53</sup> and 3.59

Å,<sup>54</sup> respectively) and are in the range of those found in reported bismuth triflate compounds (2.386(11)–3.010(3) Å).<sup>48,86</sup>

Most importantly, the P–Bi distance is 2.800(3) Å, which is only slightly longer than those in compounds A, B, and C in Figure 1 (from 2.6672(19) to 2.7696(8) Å); however, it is significantly shorter than the “pnictogen-bonded” P–Bi distances in  $\text{PS}_3\text{BiX}_3$  (3.365(1)–3.792(9) Å). The corresponding bond valences have also been calculated<sup>65,66</sup> (see Table S8 in the Supporting Information) and show that the P–Bi bond in  $[\text{PS}_3\text{Bi}]_2[\text{BOT}]$  ( $s = 0.632$  vu) is remarkably stronger than those in  $\text{PS}_3\text{BiX}_3$  ( $s = 0.137, 0.047$ , and  $0.043$  vu for  $X = \text{Cl}, \text{Br}, \text{I}$ , respectively). The sum of the bond valences at the bismuth center indicates that the Bi in  $[\text{PS}_3\text{Bi}]_2[\text{BOT}]$  ( $\sum s = 2.874$  vu) is undercoordinated in comparison to the halide analogues  $\text{PS}_3\text{BiX}_3$  ( $\sum s = 3.233, 3.217$ , and  $3.191$  vu for  $X = \text{Cl}, \text{Br}, \text{I}$ , respectively), which is in accord with the observations discussed for the gas-phase structures (*vide supra*).

We also compared the solid-state structure of  $[\text{PS}_3\text{Bi}]_2[\text{BOT}]$  to the gas-phase structure of the tricationic adduct  $[\text{PS}_3\text{Bi}]^{3+}$  obtained by DFT computations (*vide supra*). The structure corresponding to the energy minimum (in the gas phase) is not symmetrical and shows a stereochemically active lone pair at the bismuth center. Furthermore, a structure with a constrained  $C_3$  symmetry was also obtained (as a second-order saddle point) lying only 3.7 kcal/mol higher in energy. This indicates that the coordination geometry around the bismuth is very flexible and, thus, the difference between the gas-phase and solid-state structures is most likely caused by crystal-packing effects. Nevertheless, the computed P–Bi distances in the gas phase (2.697 Å for the minimum and 2.715 Å for the  $C_3$ -symmetric structure) are similar but somewhat shorter than that in the solid-state structure (2.800(3) Å). We attribute this difference to weak coordination of the triflate anions in the solid state, transferring some electron density to the bismuth center and thus elongating the P–Bi atom distance.

**2.5. Solid-State NMR Investigations.** As  $^{31}\text{P}$  NMR spectroscopy is a useful tool in studying bonding situations, we investigated specifically the compound  $[\text{PS}_3\text{Bi}]_2[\text{BOT}]$ . The chemical shifts obtained in both solid-state CP-MAS and solution  $^{31}\text{P}$  NMR spectra (+56.0 and +67.6 ppm, respectively) are similar to that of B, in which the phosphorus coordinates to a bismuth center (Figure 1,  $\delta(^{31}\text{P})$  50.8 ppm),<sup>48</sup> confirming a remarkable change in the chemical environment around the phosphorus nucleus in comparison to the free ligand  $\text{PS}_3$ ,

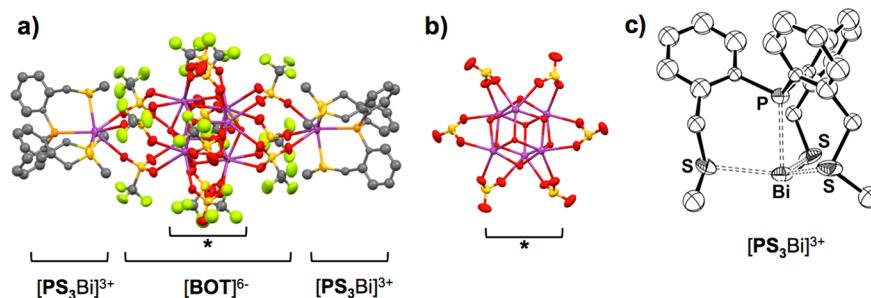
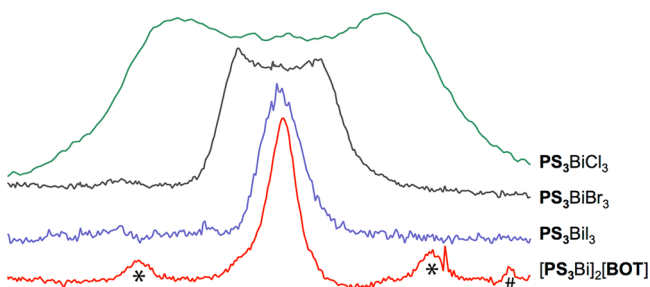


Figure 3. (a) Plot of the adduct  $[\text{PS}_3\text{Bi}]_2[\text{BOT}]$  (Bi, purple; S, yellow; P, orange; F, green; O, red; C, gray). Hydrogen atoms and solvent molecules have been omitted for clarity. (b) Side view of the section marked with asterisk in (a) showing the central core ( $\text{CF}_3$  groups are not shown). (c) ORTEP representation of the  $C_3$ -symmetric  $[\text{PS}_3\text{Bi}]^{3+}$  moiety (thermal ellipsoids are drawn at 50% probability). Hydrogen atoms, solvent molecules, and the  $[\text{BOT}]^{6-}$  cluster have been omitted for clarity. Selected atomic distances (Å): Bi–P 2.800(3), Bi–S 2.749(9), Bi–O[triflate] 2.760(1).

( $\delta(^{31}\text{P}) - 38.0 \text{ ppm}^{52}$ ). This substantial coordination chemical shift change ( $\Delta\delta \approx 100 \text{ ppm}$ ) is attributable to the significant  $\text{P} \rightarrow \text{Bi}$  charge transfer, nicely agreeing with the results of the computations (the partial charge difference between the trication  $[\text{PS}_3\text{Bi}]^{3+}$  and the ligand  $\text{PS}_3$ :  $\Delta q(\text{P}) = 0.205 \text{ e}$ ).

In the CP MAS  $^{31}\text{P}$  NMR spectra of compounds  $\text{PS}_3\text{BiX}_3$  scalar indirect spin–spin coupling between the  $^{209}\text{Bi}$  and  $^{31}\text{P}$  nuclei was observed (typically as an unresolved broad band), which is consistent with the overlap of the P and Bi lone pairs, resulting in a Mallory-type through-space coupling mechanism.<sup>87–89</sup> Furthermore, the strength of the pnictogen interaction in these compounds was found to correlate with the width of the band arising from this coupling, which increases in the order  $\text{PS}_3\text{BiI}_3 < \text{PS}_3\text{BiBr}_3 < \text{PS}_3\text{BiCl}_3$ .<sup>52</sup> Knowing that the coupling mechanism in all of these  $\text{PS}_3\text{BiX}_3$  compounds is the same, and assuming that it is the same in  $[\text{PS}_3\text{Bi}]_2[\text{BOT}]$  as well, we would expect that intensifying the interaction between P and Bi would lead to an increase in the coupling constant and as a consequence to a broadening of the band. Thus, the band of  $[\text{PS}_3\text{Bi}]_2[\text{BOT}]$  would be significantly broader than that of  $\text{PS}_3\text{BiCl}_3$ . Surprisingly, the CP MAS  $^{31}\text{P}$  NMR spectrum of  $[\text{PS}_3\text{Bi}]_2[\text{BOT}]$  (see Figure 4) exhibits a



**Figure 4.** Room-temperature solid-state CP-MAS  $^{31}\text{P}$  NMR spectra of the adduct  $[\text{PS}_3\text{Bi}]_2[\text{BOT}]$ ,  $\text{PS}_3\text{BiI}_3$ ,  $\text{PS}_3\text{BiBr}_3$ , and  $\text{PS}_3\text{BiCl}_3$  (at spinning rates of 8, 6, 6, and 10 kHz, respectively). For an easier comparison of the band widths, the resonances of  $[\text{PS}_3\text{Bi}]_2[\text{BOT}]$  and  $\text{PS}_3\text{BiX}_3$  ( $\text{X} = \text{I}, \text{Br}, \text{Cl}$ )<sup>52</sup> have been centered at the same position. For all samples the line widths of the bands have been proven to be independent from the applied spinning rates. The symbols \* and # indicate spinning side bands and  $[\text{HPS}_3]^+[\text{OTf}]^-$  impurity, respectively.

band which is narrower than that in the case of  $\text{PS}_3\text{BiI}_3$ . The remarkable half-width of 1.6 kHz for  $[\text{PS}_3\text{Bi}]_2[\text{BOT}]$  again indicates an unresolved, indirect spin–spin coupling between the  $^{31}\text{P}$  and the quadrupolar  $^{209}\text{Bi}$  nuclei. However, since the width of  $[\text{PS}_3\text{Bi}]_2[\text{BOT}]$  does not fit into the expected tendency, the coupling mechanism should be starkly different in the compounds  $\text{PS}_3\text{BiX}_3$  and  $[\text{PS}_3\text{Bi}]_2[\text{BOT}]$ . To verify this assumption, we have simulated the spin–spin coupling constant in the gas phase at the PBE1/TZ2P level with a scalar ZORA approximation (see the Supporting Information). The  $J(^{209}\text{Bi}-^{31}\text{P})$  value calculated for the gas-phase optimized structure of  $[\text{PS}_3\text{Bi}]^{3+}$  is  $-773 \text{ Hz}$ , the absolute value of which is indeed smaller than that calculated for  $\text{PS}_3\text{BiI}_3$  at the same level ( $908 \text{ Hz}^{52}$ ), agreeing with the experimental findings for the band widths. A striking difference is, however, found in the sign of the computed coupling constant, which was determined to be positive for the compounds  $\text{PS}_3\text{BiX}_3$  ( $\text{X} = \text{Cl}, \text{Br}, \text{I}$ ), while it was negative for  $[\text{PS}_3\text{Bi}]^{3+}$ . The former is characteristic for a Mallory type through-space coupling mechanism resulting from the overlap of the Bi and P lone pairs,<sup>52</sup> while we

attribute the latter to a real through-bond coupling in line with the presence of a dative  $\text{P} \rightarrow \text{Bi}$  interaction.

### 3. SUMMARY AND CONCLUSIONS

In summary, it is demonstrated that a weak secondary pnictogen interaction previously reported for  $\text{PS}_3\text{BiX}_3$  can be tuned into a dative bond employing the same molecular framework. On the basis of our DFT computations on the structures of  $[\text{PS}_3\text{BiCl}_n]^{(3-n)+}$  ( $n = 0-3$ ) and  $[\text{PS}_3\text{Bi}(\text{ACN})_3]^{3+}$  model species, the increase in covalency and thus the shift toward dative bonding can be achieved by intensifying the charge transfer from the P to the Bi center already in the case of the monocation  $[\text{PS}_3\text{BiCl}_2]^+$ . Experimentally this was realized by employing weakly coordinating triflate anions and a new coordination compound exhibiting a dative  $\text{P} \rightarrow \text{Bi}$  bond was synthesized and characterized, which shows marked contrast to pnictogen-bonded complexes  $\text{PS}_3\text{BiX}_3$  described previously. Furthermore, our investigations reveal a connection between the nature of the  $\text{P} \cdots \text{Bi}$  interaction and the spin–spin coupling mechanism between the two nuclei involved, offering the possibility to distinguish between these two types of interactions. Our results also show that ligand  $\text{P}(\text{C}_6\text{H}_4\text{-}o\text{-CH}_2\text{SCH}_3)_3$  is “flexidentate”, which means it can adopt different coordination modes and in these accordion-like complexes the distance between the bridgehead atoms may deviate by nearly  $1 \text{ \AA}$ . Therefore, this system could also be of interest for the development of new catalytic systems: for example, with transition metals.

### ■ ASSOCIATED CONTENT

#### Supporting Information

The Supporting Information is available free of charge at <https://pubs.acs.org/doi/10.1021/acs.inorgchem.0c00734>.

Description of experimental procedures, characterization of compounds, X-ray crystallographic studies, and computational details (PDF)

#### Accession Codes

CCDC 1941566 and 1941695 contain the supplementary crystallographic data for this paper. These data can be obtained free of charge via [www.ccdc.cam.ac.uk/data\\_request/cif](http://www.ccdc.cam.ac.uk/data_request/cif), or by emailing [data\\_request@ccdc.cam.ac.uk](mailto:data_request@ccdc.cam.ac.uk), or by contacting The Cambridge Crystallographic Data Centre, 12 Union Road, Cambridge CB2 1EZ, UK; fax: +44 1223 336033.

### ■ AUTHOR INFORMATION

#### Corresponding Authors

Zoltán Benkő – Budapest University of Technology and Economics, H-1111 Budapest, Hungary; [orcid.org/0000-0001-6647-8320](https://orcid.org/0000-0001-6647-8320); Email: [zbenko@mail.bme.hu](mailto:zbenko@mail.bme.hu)

Dominikus Heift – Department of Chemistry, Durham University, DH1 3LE Durham, United Kingdom; [orcid.org/0000-0002-6799-5052](https://orcid.org/0000-0002-6799-5052); Email: [dominikus.heift@durham.ac.uk](mailto:dominikus.heift@durham.ac.uk)

#### Authors

Réka Mokrai – Budapest University of Technology and Economics, H-1111 Budapest, Hungary

Jamie Barrett – Department of Chemistry, Durham University, DH1 3LE Durham, United Kingdom

David C. Apperley – Department of Chemistry, Durham University, DH1 3LE Durham, United Kingdom

Complete contact information is available at:



<https://pubs.acs.org/10.1021/acs.inorgchem.0c00734>

## Notes

The authors declare no competing financial interest.

## ACKNOWLEDGMENTS

The authors thank Dr. P. W. Dyer, Dr. D. Yufit, Dr. A. Batsanov, and Dr. G. Müller for their help and acknowledge the support of a European Union COFUND/Durham Junior Research Fellowship under EU grant agreement number 609412, the ETH Zurich, a BME-Nanotechnology FIKP grant of EMMI (BME FIKP-NAT), NKFIH (PD 116329), a Janos Bolyai Research Scholarship, a UNKP-19-4-BME-422 grant, Varga József Alapítvány, and Pro Progressio Alapítvány.

## DEDICATION

Dedicated to Prof. Magdolna Hargittai on the occasion of her 75th birthday.

## REFERENCES

- (1) Lewis, G. N. The atom and the molecule. *J. Am. Chem. Soc.* **1916**, *38* (4), 762–785.
- (2) Nandi, A.; Kozuch, S. History and Future of Dative Bonds. *Chem. - Eur. J.* **2020**, *26* (4), 759–772.
- (3) Clark, T.; Hennemann, M.; Murray, J. S.; Politzer, P. Halogen bonding: the  $\sigma$ -hole. *J. Mol. Model.* **2007**, *13* (2), 291–296.
- (4) Politzer, P.; Murray, J. S.; Concha, M. C. Sigma-hole bonding between like atoms; a fallacy of atomic charges. *J. Mol. Model.* **2008**, *14* (8), 659–665.
- (5) Politzer, P.; Murray, J. S.; Clark, T. Halogen bonding and other  $\sigma$ -hole interactions: a perspective. *Phys. Chem. Chem. Phys.* **2013**, *15* (27), 11178–11189.
- (6) Kolář, M. H.; Hobza, P. Computer Modeling of Halogen Bonds and Other  $\sigma$ -Hole Interactions. *Chem. Rev.* **2016**, *116* (9), 5155–5187.
- (7) Lim, J. Y. C.; Beer, P. D. Sigma-Hole Interactions in Anion Recognition. *Chem.* **2018**, *4* (4), 731–783.
- (8) Moilanen, J.; Ganesamoorthy, C.; Balakrishna, M. S.; Tuononen, H. M. Weak Interactions between Trivalent Pnictogen Centers: Computational Analysis of Bonding in Dimers  $X_3E \cdots EX_3$  ( $E$  = Pnictogen,  $X$  = Halogen). *Inorg. Chem.* **2009**, *48* (14), 6740–6747.
- (9) Zahn, S.; Frank, R.; Hey-Hawkins, E.; Kirchner, B. Pnictogen Bonds: A New Molecular Linker? *Chem. - Eur. J.* **2011**, *17* (22), 6034–6038.
- (10) Scheiner, S. The Pnictogen Bond: Its Relation to Hydrogen, Halogen, and Other Noncovalent Bonds. *Acc. Chem. Res.* **2013**, *46* (2), 280–288.
- (11) Desiraju, G. R.; Ho, P. S.; Kloo, L.; Legon, A. C.; Marquardt, R.; Metrangola, P.; Politzer, P.; Resnati, G.; Rissanen, K. Definition of the halogen bond (IUPAC Recommendations 2013). *Pure Appl. Chem.* **2013**, *85* (8), 1711–1713.
- (12) Scheiner, S. *Noncovalent forces*; Springer International: Cham, Switzerland, 2015; online resource.
- (13) Moaven, S.; Yu, J.; Vega, M.; Unruh, D. K.; Cozzolino, A. F. Self-assembled reversed bilayers directed by pnictogen bonding to form vesicles in solution. *Chem. Commun.* **2018**, *54* (64), 8849–8852.
- (14) Schmauck, J.; Breugst, M. The potential of pnictogen bonding for catalysis – a computational study. *Org. Biomol. Chem.* **2017**, *15* (38), 8037–8045.
- (15) Benz, S.; Poblador-Bahamonde, A. I.; Low-Ders, N.; Matile, S. Catalysis with Pnictogen, Chalcogen, and Halogen Bonds. *Angew. Chem., Int. Ed.* **2018**, *57* (19), 5408–5412.
- (16) Tang, Q. J.; Li, Q. Z. Enhancing effect of metal coordination interaction on pnictogen bonding. *J. Mol. Model.* **2016**, *22* (3), 1–7.
- (17) Mahmudov, K. T.; Gurbanov, A. V.; Guseinov, F. I.; da Silva, M. F. C. G. Noncovalent interactions in metal complex catalysis. *Coord. Chem. Rev.* **2019**, *387*, 32–46.
- (18) Moaven, S.; Andrews, M. C.; Polaske, T. J.; Karl, B. M.; Unruh, D. K.; Bosch, E.; Bowling, N. P.; Cozzolino, A. F. Triple-Pnictogen Bonding as a Tool for Supramolecular Assembly. *Inorg. Chem.* **2019**, *58* (23), 16227–16235.
- (19) Scilabra, P.; Terraneo, G.; Daolio, A.; Baggioli, A.; Famulari, A.; Leroy, C.; Bryce, D. L.; Resnati, G. 4,4'-Dipyridyl Dioxide-SbF<sub>3</sub> Cocrystal: Pnictogen Bond Prevails over Halogen and Hydrogen Bonds in Driving Self-Assembly. *Cryst. Growth Des.* **2020**, *20* (2), 916–922.
- (20) Lu, L.; Lu, Y.; Zhu, Z.; Liu, H. Pnictogen, chalcogen, and halogen bonds in catalytic systems: theoretical study and detailed comparison. *J. Mol. Model.* **2020**, *26* (1), 16.
- (21) Yang, M. X.; Hirai, M.; Gabbai, F. P. Phosphonium-stibonium and bis-stibonium cations as pnictogen-bonding catalysts for the transfer hydrogenation of quinolines. *Dalton Trans.* **2019**, *48* (20), 6685–6689.
- (22) Legon, A. C. Tetrel, pnictogen and chalcogen bonds identified in the gas phase before they had names: a systematic look at non-covalent interactions. *Phys. Chem. Chem. Phys.* **2017**, *19* (23), 14884–14896.
- (23) Klinkhammer, K. W.; Pyykko, P. Ab Initio Interpretation of the Closed-Shell Intermolecular E $\cdots$ E Attraction in Dipnictogen (H<sub>2</sub>E-EH<sub>2</sub>)<sub>2</sub> and Dichalcogen (HE-EH)<sub>2</sub> Hydride Model Dimers. *Inorg. Chem.* **1995**, *34* (16), 4134–4138.
- (24) Oliveira, V.; Kraka, E. Systematic Coupled Cluster Study of Noncovalent Interactions Involving Halogens, Chalcogens, and Pnictogens. *J. Phys. Chem. A* **2017**, *121* (49), 9544–9556.
- (25) Setiawan, D.; Kraka, E.; Cremer, D. Strength of the Pnictogen Bond in Complexes Involving Group Va Elements N, P, and As. *J. Phys. Chem. A* **2015**, *119* (9), 1642–1656.
- (26) Setiawan, D.; Kraka, E.; Cremer, D. Description of pnictogen bonding with the help of vibrational spectroscopy-The missing link between theory and experiment. *Chem. Phys. Lett.* **2014**, *614*, 136–142.
- (27) Marin-Luna, M.; Alkorta, I.; Elguero, J. A computational study on [(PH<sub>2</sub>X)(2)](+) homodimers involving intermolecular two-center three-electron bonds. *Struct. Chem.* **2016**, *27* (3), 753–762.
- (28) Roohi, H.; Tondro, T. Exploring the pnictogen bond non-covalent interactions in 4-XPhNH<sub>2</sub>:PFnH<sub>3</sub>-n complexes (n = 1–3, X = H, F, CN, CHO, NH<sub>2</sub>, CH<sub>3</sub>, NO<sub>2</sub> and OCH<sub>3</sub>). *J. Fluorine Chem.* **2017**, *202*, 19–33.
- (29) Trubenstein, H. J.; Moaven, S.; Vega, M.; Unruh, D. K.; Cozzolino, A. F. Pnictogen bonding with alkoxide cages: which pnictogen is best? *New J. Chem.* **2019**, *43* (36), 14305–14312.
- (30) Radha, A.; Kumar, S.; Sharma, D.; Jassal, A. K.; Zareba, J. K.; Franconetti, A.; Frontera, A.; Sood, P.; Pandey, S. K. Indirect influence of alkyl substituent on sigma-hole interactions: The case study of antimony(III) diphenyldithiophosphates with covalent Sb-S and non-covalent Sb center dot center dot center dot S pnictogen bonds. *Polyhedron* **2019**, *173*, 114126.
- (31) Tondro, T.; Roohi, H. Substituent effects on the halogen and pnictogen bonds characteristics in ternary complexes 4-YPhNH<sub>2</sub>  $\cdots$  PH<sub>2</sub>F  $\cdots$  ClX (Y = H, F, CN, CHO, NH<sub>2</sub>, CH<sub>3</sub>, NO<sub>2</sub> and OCH<sub>3</sub>, and X = F, OH, CN, NC, FCC and NO<sub>2</sub>): A theoretical study. *J. Chem. Sci.* **2020**, *132* (1), 1–21.
- (32) Shukla, R.; Chopra, D. Pnictogen bonds or “chalcogen bonds”: exploiting the effect of substitution on the formation of P $\cdots$ Se noncovalent bonds. *Phys. Chem. Chem. Phys.* **2016**, *18* (20), 13820–13829.
- (33) Wysokiński, R.; Zierkiewicz, W.; Michalczyk, M.; Scheiner, S. How Many Pnictogen Bonds can be Formed to a Central Atom Simultaneously? *J. Phys. Chem. A* **2020**, *124*, 2046.
- (34) Zierkiewicz, W.; Michalczyk, M.; Wysokiński, R.; Scheiner, S. On the ability of pnictogen atoms to engage in both  $\sigma$  and  $\pi$ -hole complexes. Heterodimers of ZF(2)C(6)H(5) (Z = P, As, Sb, Bi) and NH<sub>3</sub>. *J. Mol. Model.* **2019**, *25* (6), 1–13.
- (35) Esrafil, M. D.; Vakili, M.; Solimannejad, M. Cooperative effects in pnictogen bonding: (PH<sub>2</sub>F)<sub>2</sub>–7 and (PH<sub>2</sub>Cl)<sub>2</sub>–7 clusters. *Chem. Phys. Lett.* **2014**, *609*, 37–41.

- (36) Adhikari, U.; Scheiner, S. Comparison of P ... D (D = P,N) with other noncovalent bonds in molecular aggregates. *J. Chem. Phys.* **2011**, *135* (18), 184306.
- (37) Scheiner, S. Comparison of halide receptors based on H, halogen, chalcogen, pnictogen, and tetrel bonds. *Faraday Discuss.* **2017**, *203*, 213–226.
- (38) Scheiner, S.; Michalczyk, M.; Zierkiewicz, W. Structures of clusters surrounding ions stabilized by hydrogen, halogen, chalcogen, and pnictogen bonds. *Chem. Phys.* **2019**, *524*, 55–62.
- (39) Scheiner, S.; Michalczyk, M.; Wysokinski, R.; Zierkiewicz, W. Structures and energetics of clusters surrounding diatomic anions stabilized by hydrogen, halogen, and other noncovalent bonds. *Chem. Phys.* **2020**, *530*, 110590.
- (40) Scheiner, S. Effects of Substituents upon the P...N Noncovalent Interaction: The Limits of Its Strength. *J. Phys. Chem. A* **2011**, *115* (41), 11202–11209.
- (41) Buzsáki, D.; Kelemen, Z.; Nyulászi, L. Stretching the P–C Bond. Variations on Carbenes and Phosphanes. *J. Phys. Chem. A* **2020**, *124*, 2660.
- (42) Joshi, P. R.; Ramanathan, N.; Sundararajan, K.; Sankaran, K. Phosphorous bonding in  $\text{PCl}_3\text{:H}_2\text{O}$  adducts: A matrix isolation infrared and ab initio computational studies. *J. Mol. Spectrosc.* **2017**, *331*, 44–52.
- (43) Zong, J.; Mague, J. T.; Kraml, C. M.; Pascal, R. A. A Congested in,in-Diphosphine. *Org. Lett.* **2013**, *15* (9), 2179–2181.
- (44) Joshi, P. R.; Ramanathan, N.; Sundararajan, K.; Sankaran, K. Evidence for Phosphorus Bonding in Phosphorus Trichloride-Methanol Adduct: A Matrix Isolation Infrared and ab Initio Computational Study. *J. Phys. Chem. A* **2015**, *119* (14), 3440–3451.
- (45) Xu, Y.; Szell, P. M. J.; Kumar, V.; Bryce, D. L. Solid-state NMR spectroscopy for the analysis of element-based non-covalent interactions. *Coord. Chem. Rev.* **2020**, *411*, 213237.
- (46) Hupf, E.; Lork, E.; Mebs, S.; Checinska, L.; Beckmann, J. Probing Donor-Acceptor Interactions in pen-Substituted Diphenylphosphinoacenaphthyl-Element Dichlorides of Group 13 and 15 Elements. *Organometallics* **2014**, *33* (24), 7247–7259.
- (47) Nejman, P. S.; Curzon, T. E.; Bühl, M.; McKay, D.; Woollins, J. D.; Ashbrook, S. E.; Cordes, D. B.; Slawin, A. M. Z.; Kilian, P. Phosphorus–Bismuth Peri-Substituted Acenaphthenes: A Synthetic, Structural, and Computational Study. *Inorg. Chem.* **2020**, *59*, 5616.
- (48) Chitnis, S. S.; Burford, N.; Decken, A.; Ferguson, M. J. Coordination Complexes of Bismuth Triflates with Tetrahydrofuran and Diphosphine Ligands. *Inorg. Chem.* **2013**, *52* (12), 7242–7248.
- (49) Wielandt, J. W.; Petrie, S.; Kilah, N. L.; Willis, A. C.; Dewhurst, R. D.; Belaj, F.; Orthaber, A.; Stranger, R.; Wild, S. B. Self-Assembly of Square-Planar Halide Complexes of Trimethylphosphine-Stabilized Diphenyl-Arsenium, -Stibonium, and -Bismuthenium Hexafluorophosphates. *Aust. J. Chem.* **2016**, *69* (5), 524–532.
- (50) Kilah, N. L.; Petrie, S.; Stranger, R.; Wielandt, J. W.; Willis, A. C.; Wild, S. B. Triphenylphosphine-Stabilized Diphenyl-Arsenium, -Stibonium, and -Bismuthenium Salts. *Organometallics* **2007**, *26* (25), 6106–6113.
- (51) Chalmers, B. A.; Meigh, C. B. E.; Nejman, P. S.; Bühl, M.; Lébl, T.; Woollins, J. D.; Slawin, A. M. Z.; Kilian, P. Geminally Substituted Tris(acenaphthyl) and Bis(acenaphthyl) Arsines, Stibines, and Bismuthine: A Structural and Nuclear Magnetic Resonance Investigation. *Inorg. Chem.* **2016**, *55* (14), 7117–7125.
- (52) Mokrai, R.; Barrett, J.; Apperley, D. C.; Batsanov, A. S.; Benkő, Z.; Heift, D. Weak Pnictogen Bond with Bismuth: Experimental Evidence Based on Bi–P Through-Space Coupling. *Chem. - Eur. J.* **2019**, *25* (16), 4017–4024.
- (53) Cordero, B.; Gomez, V.; Platero-Prats, A. E.; Reves, M.; Echeverria, J.; Cremades, E.; Barragan, F.; Alvarez, S. Covalent radii revisited. *Dalton Trans.* **2008**, *21*, 2832–2838.
- (54) Mantina, M.; Chamberlin, A. C.; Valero, R.; Cramer, C. J.; Truhlar, D. G. Consistent van der Waals Radii for the Whole Main Group. *J. Phys. Chem. A* **2009**, *113* (19), 5806–5812.
- (55) Clardy, J. C.; Milbrath, D. S.; Springer, J. P.; Verkade, J. G. Characterization and molecular structure of 1-hydro-2,8,9-trioxa-1-phospha-5-aza-tricyclo[3.3.3.0]undecane tetrafluoroborate. Penta-coordination of phosphorus. *J. Am. Chem. Soc.* **1976**, *98* (2), 623–624.
- (56) Verkade, J. G. Main-Group Atranes - Chemical and Structural Features. *Coord. Chem. Rev.* **1994**, *137*, 233–295.
- (57) Nyulaszi, L.; Veszpremi, T.; DSa, B. A.; Verkade, J. Photoelectron spectra and structures of proazaphosphatranes. *Inorg. Chem.* **1996**, *35* (21), 6102–6107.
- (58) Liu, X.; Bai, Y.; Verkade, J. G. Synthesis and structural features of new sterically hindered azaphosphatranes systems: ZP-(RNCH<sub>2</sub>CH<sub>2</sub>)(3)N. *J. Organomet. Chem.* **1999**, *582* (1), 16–24.
- (59) Suter, R.; Swidan, A. a.; Macdonald, C. L. B.; Burford, N. Oxidation of a germanium(II) dication to access cationic germanium(IV) fluorides. *Chem. Commun.* **2018**, *54* (33), 4140–4143.
- (60) Swidan, A.; Suter, R.; Macdonald, C. L. B.; Burford, N. Tris(benzoimidazol)amine (L) complexes of pnictogen(III) and pnictogen(V) cations and assessment of the [LP]<sub>3</sub><sup>+</sup>/[LPF<sub>2</sub>]<sub>3</sub><sup>+</sup> redox couple. *Chem. Sci.* **2018**, *9* (26), 5837–5841.
- (61) Green, J. P.; Wells, J. A. L.; Orthaber, A. Heavier pnictogens – treasures for optical electronic and reactivity tuning. *Dalton Trans.* **2019**, *48* (14), 4460–4466.
- (62) Weigand, J. J.; Feldmann, K.-O.; Echterhoff, A. K. C.; Ehlers, A. W.; Lammertsma, K. Preparation of Ligand-Stabilized [P<sub>4</sub>O<sub>4</sub>]<sup>2+</sup> by Controlled Hydrolysis of a Janus Head Type Diphosphorus Trication. *Angew. Chem., Int. Ed.* **2010**, *49* (35), 6178–6181.
- (63) Šimon, P.; de Proft, F.; Jambor, R.; Růžicka, A.; Dostál, L. Monomeric Organoantimony(I) and Organobismuth(I) Compounds Stabilized by an NCN Chelating Ligand: Syntheses and Structures. *Angew. Chem., Int. Ed.* **2010**, *49* (32), 5468–5471.
- (64) Kremláček, V.; Hyvl, J.; Yoshida, W. Y.; Růžicka, A.; Rheingold, A. L.; Turek, J.; Hughes, R. P.; Dostál, L.; Cain, M. F. Heterocycles Derived from Generating Monovalent Pnictogens within NCN Pincers and Bidentate NC Chelates: Hypervalency versus Bell-Clappers versus Static Aromatics. *Organometallics* **2018**, *37* (15), 2481–2490.
- (65) Brown, I. D. VALENCE: A program for calculating bond valences. *J. Appl. Crystallogr.* **1996**, *29*, 479–480.
- (66) Brese, N. E.; O'Keeffe, M. Bond-Valence Parameters for Solids. *Acta Crystallogr., Sect. B: Struct. Sci.* **1991**, *47*, 192–197.
- (67) Glendenning, E. D.; Reed, A. E.; Carpenter, J. E.; Bohmann, J. A.; Morales, C. M.; Weinhold, F. NBO 5.0.; Theoretical Chemistry Institute, University of Wisconsin: Madison, WI, 2001.
- (68) Bader, R. F. W. A quantum theory of molecular structure and its applications. *Chem. Rev.* **1991**, *91* (5), 893–928.
- (69) Cremer, D.; Kraka, E. Chemical-Bonds without Bonding Electron-Density - Does the Difference Electron-Density Analysis Suffice for a Description of the Chemical-Bond. *Angew. Chem., Int. Ed. Engl.* **1984**, *23* (8), 627–628.
- (70) Cremer, D.; Kraka, E. A Description of the Chemical-Bond in Terms of Local Properties of Electron-Density and Energy. *Croat. Chem. Acta* **1984**, *57* (6), 1259–1281.
- (71) Riddlestone, I. M.; Kraft, A.; Schaefer, J.; Krossing, I. Taming the Cationic Beast: Novel Developments in the Synthesis and Application of Weakly Coordinating Anions. *Angew. Chem., Int. Ed.* **2018**, *57* (43), 13982–14024.
- (72) Ollevier, T. New trends in bismuth-catalyzed synthetic transformations. *Org. Biomol. Chem.* **2013**, *11* (17), 2740–2755.
- (73) Ollevier, T. Bismuth-Mediated Organic Reactions. *Top. Curr. Chem.* **2012**, *311*, 1–277.
- (74) Labrouillere, M.; Le Roux, C.; Gaspard, H.; Laporterie, A.; Dubac, J.; Desmurs, J. R. An efficient method for the preparation of bismuth(III) trifluoromethanesulfonate. *Tetrahedron Lett.* **1999**, *40* (2), 285–286.
- (75) Gaspard-loughmane, H.; Le Roux, C. Bismuth(III) triflate in organic synthesis. *Eur. J. Org. Chem.* **2004**, *2004* (12), 2517–2532.
- (76) Chitnis, S. S.; Vos, K. A.; Burford, N.; McDonald, R.; Ferguson, M. J. Distinction between coordination and phosphine ligand oxidation: interactions of di- and triphosphines with Pn(3+) (Pn = P, As, Sb, Bi). *Chem. Commun.* **2016**, *52* (4), 685–688.



(77) Loera Fernandez, I. I.; Donaldson, S. L.; Schipper, D. E.; Andleeb, S.; Whitmire, K. H. Anionic Bismuth-Oxido Carboxylate Clusters with Transition Metal Counteranions. *Inorg. Chem.* **2016**, *55* (21), 11560–11569.

(78) Dehnen, S.; Corrigan, J. F. *Clusters - contemporary insight in structure and bonding*; Springer International: Cham, Switzerland, 2017; p 379.

(79) Senevirathna, D. C.; Blair, V. L.; Werrett, M. V.; Andrews, P. C. Polynuclear Bismuth Oxido Sulfonate Clusters, Polymers, and Ion Pairs from Bi<sub>2</sub>O<sub>3</sub> under Mild Conditions. *Inorg. Chem.* **2016**, *55* (21), 11426–11433.

(80) Senevirathna, D. C.; Werrett, M. V.; Blair, V. L.; Mehring, M.; Andrews, P. C. 2D and 3D Coordination Networks of Polynuclear Bismuth Oxido/Hydroxido Sulfonate Clusters from Low Temperature Solid-State Metathesis Reactions. *Chem. - Eur. J.* **2018**, *24* (26), 6722–6726.

(81) Rogow, D. L.; Fei, H. H.; Brennan, D. P.; Ikehata, M.; Zavalij, P. Y.; Oliver, A. G.; Oliver, S. R. J. Hydrothermal Synthesis of Two Cationic Bismuthate Clusters: An Alkylendisulfonate Bridged Hexamer, [Bi<sub>6</sub>O<sub>4</sub>(OH)(4)(H<sub>2</sub>O)(2)][(CH<sub>2</sub>)(2)(SO<sub>3</sub>)(2)](3) and a Rare Nonamer Templated by Triflate, [Bi<sub>9</sub>O<sub>8</sub>(OH)(6)][CF<sub>3</sub>SO<sub>3</sub>](5). *Inorg. Chem.* **2010**, *49* (12), 5619–5624.

(82) Pye, C. C.; Gunasekara, C. M.; Rudolph, W. W. An ab initio investigation of bismuth hydration. *Can. J. Chem.* **2007**, *85* (11), 945–950.

(83) Sundvall, B. Crystal and Molecular-Structure of Tetraoxotetrahydroxobismuth(III) Nitrate Monohydrate, Bi<sub>6</sub>O<sub>4</sub>(HO)<sub>4</sub>(NO<sub>3</sub>)<sub>6</sub>·H<sub>2</sub>O. *Acta Chem. Scand. A* **1979**, *33* (3), 219–224.

(84) Sattler, D.; Schlesinger, M.; Mehring, M.; Schalley, C. A. Mass Spectrometry and Gas-Phase Chemistry of Bismuth-Oxido Clusters. *ChemPlusChem* **2013**, *78* (9), 1005–1014.

(85) Srinivas, K.; Sathyanarayana, A.; Babu, C. N.; Prabusankar, G. Bismuth(III)dichalcogenones as highly active catalysts in multiple C–C bond formation reactions. *Dalton Trans.* **2016**, *45* (12), 5196–5209.

(86) Mazieres, S.; Le Roux, C.; Peyronneau, M.; Gornitzka, H.; Roques, N. Structural characterization of bismuth(III) and antimony(III) chlorotriflates: Key intermediates in catalytic Friedel-Crafts transformations. *Eur. J. Inorg. Chem.* **2004**, *2004* (14), 2823–2826.

(87) Mallory, F. B.; Luzik, E. D.; Mallory, C. W.; Carroll, P. J. Nuclear spin-spin coupling via nonbonded interactions. 7. Effects of molecular structure on nitrogen-fluorine coupling. *J. Org. Chem.* **1992**, *57* (1), 366–370.

(88) Manatt, S. L.; Cooper, M. A.; Mallory, C. W.; Mallory, F. B. Evidence for a Steric Effect on Directly Bonded Carbon-Fluorine and Carbon-Proton Nuclear Magnetic-Resonance Couplings. *J. Am. Chem. Soc.* **1973**, *95* (3), 975–977.

(89) Hierso, J.-C.; Fihri, A.; Ivanov, V. V.; Hanquet, B.; Pirio, N.; Donnadieu, B.; Rebière, B.; Amardeil, R.; Meunier, P. “Through-Space” Nuclear Spin–Spin JPP Coupling in Tetrakisphosphine Ferrocenyl Derivatives: A <sup>31</sup>P NMR and X-ray Structure Correlation Study for Coordination Complexes. *J. Am. Chem. Soc.* **2004**, *126* (35), 11077–11087.